Sharpening of directional selectivity from neural output of rabbit retina

Aurel Vasile Martiniuc · Alois Knoll

Abstract The estimation of motion direction from time varying retinal images is a fundamental task of visual systems. Neurons that selectively respond to directional visual motion are found in almost all species. In many of them already in the retina direction selective neurons signal their preferred direction of movement. Scientific evidences suggest that direction selectivity is carried from the retina to higher brain areas. Here we adopt a simple integrate-and-fire neuron model, inspired by recent work of Casti et al. (2008), to investigate how directional selectivity changes in cells postsynaptic to directional selective retinal ganglion cells (DSRGC). Our model analysis shows that directional selectivity in the postsynaptic cells increases over a wide parameter range. The degree of directional selectivity positively correlates with the probability of burst-like firing of presynaptic DSRGCs. Postsynaptic potentials summation and spike threshold act together as a temporal filter upon the input spike train. Prior to the intricacy of neural circuitry between retina and higher brain areas, we suggest that sharpening is a straightforward result of the intrinsic spiking pattern of the DSRGCs combined with the summation of excitatory postsynaptic potentials and the spike threshold in postsynaptic neurons.

Action Editor: Catherine E. Carr

A. V. Martiniuc (✉) · A. Knoll
Computer Science Department VI, Technical University Munich,
85748 Garching, Germany
e-mail: martiniv@in.tum.de

A. Knoll
e-mail: knoll@in.tum.de

Abbreviations

DSRGC	direction selective retinal ganglion cell
LGN	lateral geniculate nucleus
SPN	simulated postsynaptic neuron
EPSP	excitatory postsynaptic potential
IPSP	inhibitory postsynaptic potential
DSi	Directional Selectivity index
AHP	After-Hyperpolarization
TFR	(spike) transfer ratio
iS	Index of sharpening
AOS	Accessory Optic System

1 Introduction

As early as in the mammalian retina the motion perception is signaled toward higher brain areas by so-called direction selective ganglion cells (DSRGCs). These cells signal stimulus motion in a preferred direction and are silent to movement in the opposite, null direction.

DSRGCs have been extensively characterized in the rabbit retina (Barlow et al. 1964; Barlow et al. 1965; Vaney et al. 1981b; Levick 1967; Devries and Baylor 1997) but occur in many other species as well: mouse (Weng et al. 2005; Kim et al. 2008; Huberman et al. 2009), cat (Stanford and Sherman 1984), rat (Dann and Buhl 1987), turtle (Jensen and Devoe 1983), ground squirrel (Michael 1966) and teleost fish (Damjanovic et al. 2009).

Retinal direction selective cells can be separated in ON-OFF cells—if they respond at the beginning and the end of an incremental or decremental light stimulus—and in ON cells—if

they respond at the beginning of an incremental light stimulus only. In the mouse retina a new OFF direction selective cell type has been recently discovered (Kim et al. 2008). The ON-OFF and ON cell types send the directional information to different nuclei: the ON-OFF DS cells project to the dorsal lateral geniculate nucleus and the superior colliculus (Cleland et al. 1976; Vaney et al. 1981a). The ON DS cells represent the main input to the Accessory Optic System (AOS, Buhl and Peichl 1986; Ackert et al. 2006; He and Masland 1998; Oyster 1968; Amthor et al. 1989; Pu and Amthor 1990; Yonehara et al. 2009). The functional properties of cells in the accessory optic system are consistent with their input from ON-DS cells in many species including primates: cat (Grasse et al. 1984), rat (van der Togt et al. 1993), and primates (Mustari and Fuchs 1989; Hoffmann and Distler 1989). A study performed in the rabbit's dorsal geniculate nucleus (Levick et al. 1969) reports a higher directional selectivity for LGN neurons compared to retinal ON-OFF DSRGCs. It remained unclear, however, how the sharpening of directional selectivity may be achieved. Directional selective cells in higher brain areas are rarely recorded in contrast to the abundant putative presynaptic DSRGCs (however, in cat DSRGCs are rarely encountered too, Cleland and Lewick 1974).

In this study we took advantage of simultaneously recorded DSRGCs (both ON-OFF and ON DS) and asked under what conditions neurons postsynaptic to the DSRGC provide a more accurate directional tuning than the presynaptic cells. We investigated in our simulations, monosynaptic connections where the recorded spike train of a single DSRGC provides the presynaptic input to a postsynaptic model neuron. We also tested how polysynaptic inputs arrangements, from multiple DSRGCs, act upon the directional tuning at postsynaptic target.

Recently, Casti (Casti et al. 2008) demonstrated that using a simple approach, consisting in recorded retinal spikes, a variant of leaky integrate-and-fire model (firstly introduced by Wörgötter and Koch 1991) and excluding the diverse array of ion channels involved at retinogeniculate synapse and any feedback inputs, there is no need for any special synaptic mechanism beyond simple summation of EPSPs, necessary to accurately simulate the LGN discharge. Carandini, used a similar approach (he used a voltage based model instead a conductance based one) to indicate that "thalamic integration of spikes from the dominant retinal input depends primarily on postsynaptic summation and on basic mechanism of spike generation" (Carandini et al. 2007). Therefore, we adopted a simple integrate-and-fire model that has been validated recently for the retinogeniculate pathway of the cat and proposed for a general use (Casti et al. 2008) in the same simple manner as described above (without taking into account neither synaptic plasticity nor feedback inputs), and asked

how directional tuning is modified at postsynaptic level to DSRGCs. We also tried to give an explanation for the sharpening in DS observed under these conditions, based on intrinsic property of one type of DSRGC. We have explored all the parameters involved, under the physiological plausible range. Apparently, at presynaptic stage, the key role is played by burst-like activity in the ON-OFF DSRGCs while at postsynaptic stage the most important parameters are the height of the spike threshold relative to the PSP amplitude and the postsynaptic cell's time constant.

The simulated postsynaptic neuron (SPN) receives excitatory input and, in some simulations, also inhibitory input from its retinal presynaptic partners. We show that sharpening of directional tuning occurs over a wide range of biophysically reasonable parameters for ON-OFF direction selective cells but less so for ON direction selective cells. To explain the discrepancy we characterized the spike train properties of the two cell types. We found that burst-like activity, which is more accentuated in one cell type (ON-OFF DSRGC), is one of the key factors responsible for the broad parameter range that lead to directional sharpening. Burst-like activity commonly found in ON-OFF DSRGCs apparently carries the information regarding the direction of stimulus motion. Additionally, the main effect responsible for the enhancement of direction-selectivity is presumably the spike threshold for the integrate-and-fire model, i.e. the SPN has a selective reduction in gain for input spike trains with long intervals, and an increase in gain for short intervals. Similar previous research efforts have also indicated that spike threshold at postsynaptic level substantially contributes to sharpening of direction selectivity in cat primary visual cortex (Jagadeesh et al. 1997; Carandini and Ferster 2000; Volgushev et al. 2000; Priebe and Ferster 2005).

Furthermore, we investigate a hypothetical case of model neurons that receive direction selective input from multiple DSRGCs. The parameter range describing the strength of presynaptic excitatory input is shifted toward lower values, in order to achieve sharpening in directional tuning at the SPN. Past a specific strength of presynaptic excitatory conductance, if two strong excitatory inputs from two cells tuned to the same direction arrive simultaneously at the (Vaney et al. 1981 please cite also Levick 1967; Devries and Baylor 1997) same postsynaptic neuron, almost every EPSP will give rise to an action potential (AP) at the postsynaptic neuron and no sharpening in direction selectivity can be achieved under our simulation conditions. We also found that a SPN receiving convergent excitatory input from two DSRGCs with the same preferred direction will signal better the direction of the stimulus motion than if the two DSRGCs would hold opposite preferred directions.

2 Methods

2.1 Experimental data

We used data recorded from retinal ganglion cells of the adult isolated rabbit retina. The data acquisition using a 60 channel multi-electrode array (Multichannelsystems, Reutlingen, Germany) and off-line analysis has been described in (Zeck and Masland 2007).

Direction selectivity was tested using a square wave spatial grating moved in $N=8$ equally separated directions $\varphi_i = i \cdot \frac{2\pi}{N}$, $i=0,1,...,N-1$. For each direction the grating (spatial frequency 1 cycles/mm) was presented for 7 s at a temporal frequency of 1 Hz followed by a stimulus free interval of the same length. The total stimulus length ranged from 600 s to 1,200 s. The spatial extent of the moving grating was ~7 μm^2 on the retina. Thus, multiple cells were stimulated and recorded simultaneously.

Individual tuning curves were obtained considering the firing rate of each cell for each of the eight equidistant directions. Data from 10 ON-OFF DSRGCs and from 3 ON DSRGCs were used in this study.

2.2 Direction selectivity index

To quantify the directional tuning of a neuron, we used the direction selectivity index (DSi) as described by Taylor and Vaney (2002),

$$DSi = \frac{\left\| \sum_i \vec{v}_i \right\|}{\sum_i r_i}, \quad \vec{v}_i = r_i \begin{pmatrix} \cos \varphi_i \\ \sin \varphi_i \end{pmatrix}. \qquad (1)$$

$\vec{v}_i$ is a vector pointing in the direction of the stimulus with the length equal to the number of spikes recorded during presentation of the stimulus (r_i). The DSi explains the directional tuning based on the firing rates for different particular movement directions of the visual stimulus. The minimum value of 0 characterizes a non-directional neuron whereas the maximum value of 1 characterizes a neuron that responds for a single direction of movement. The higher the DSi the higher direction selectivity is.

2.3 Measure of burst-like activity

In order to have a better understanding of the mechanism that presumably underlies the sharpening in direction selectivity of neurons postsynaptic to DSRGCs, we evaluated the burst-like firing of DSRGCs and postsynaptic model neurons. Burst-like firing events were defined as (at least two) spikes occurring after a prolonged period of silence, i.e. inter spike interval (ISI) larger than 50 ms, followed by an ISI shorter than 5 ms (Godwin et al. 1996; Guido et al. 1995; Lu et al.

1992). Burst rate r^{burst} was defined as the number of burst-like firing events per time. Thus, we scanned the spike train of each cell (10 ON-OFF DSRGC and 3 ON DSRGC) for each stimulus direction (8 different directions) and each stimulus repetition (7 stimulus repetitions at each direction). The burst rate was then quantified as total number of calculated bursts divided by total duration of stimulus presentation for each cell.

To further investigate the role of presynaptic property (i.e. burst-like activity) we calculated the index of directional selectivity from burst rates (DSi^{burst}) in the same manner as from firing rates in response to stimulus presented at 8 different directions of movement.

$$DSi^{burst} = \frac{\left\| \sum_i \vec{v}_i^{burst} \right\|}{\sum_i r_i^{burst}}, \quad \vec{v}_i^{burst} = r_i^{burst} \begin{pmatrix} \cos \varphi_i \\ \sin \varphi_i \end{pmatrix}. \qquad (2)$$

Once that we identified the bursts in presynaptic spike trains, we asked how many APs in the postsynaptic spike trains are at origin a spike within a presynaptic burst-like event. Thus, we were able to separate in the postsynaptic spike trains those APs originating in burst-like firing in the DSRGCs from the other postsynaptic APs and to see the contribution of burst-like activity in the presynaptic neurons over the edited postsynaptic spike trains.

Further, we quantified the influence of the presynaptic burst-like activity in editing the corresponding SPN spike trains.

In this sense, for all pre- and postsynaptic pairs, we counted every postsynaptic AP with timing higher than 0 ms and lower than 5 ms (Kara and Reid 2003; Usrey 2002; Bair 1999) comparing with timing of each spike within a burst of its presynaptic counterpart. Those spikes in SPN trains were accounted as originating in a burst of presynaptic spikes. We defined burst efficacy (B^e) as the number of spikes at the SPN, at the preferred stimulus direction, evoked by burst-like activity of the DSRGC divided by the total number of spikes at the SPN, at preferred direction.

$$B^e = \frac{\#\text{SPN spikes due to bursts (at preferred direction)}}{\#\text{SPN spikes (at preferred direction)}}$$

$$\qquad (3)$$

where "#" stands for "number of".

To quantify the directional tuning of the activity in the SPN due to burst-like activity in the presynaptic cell, after we identified the number of APs in the SPN trains having at origin a presynaptic burst, we calculated the index of directional selectivity at SPN due to presynaptic burst-like activity (DSi SPN^{burst}) in the same manner as from firing rates in Eq. (1).

2.4 Modeling postsynaptic neurons

For modeling neurons postsynaptic to DSRGCs, we used a conductance-based "integrate and fire" (I&F) neuron

model that had originally been introduced by Wörgötter and Koch (1991). A variant of this model was used by Casti et al. (2008) to describe the response of LGN neurons to input from retinal ganglion cells (RGCs). The membrane potential $V(t)$ of the I&F neuron is governed by

$$C_m \frac{dV}{dt} = -(V - V_{rest})g_m - (V - E_a) \sum_f g_a(t - t_f)$$
$$- (V - E_e) \sum_s g_e(t - t_s). \qquad (4)$$

An action potential is generated whenever the membrane reaches the threshold V_{thresh} (Fig. 1). The first term on the right side of Eq. (4) describes the leakage current while the second term describes the effect of afterhyperpolarization (AHP) following each action potential. The input of the neuron is provided through excitatory channels (third term on right side) resulting in EPSPs. In a single case, we also considered "locked inhibition", i.e. inhibition that follows excitation with a fixed delay Δt_{ie} (see section 3.1, Fig. 3 (b)), and an additional inhibitory current $-(V - E_i) \sum_s g_i(t - t_s - \Delta t_{ie})$ was added.

The time-dependent conductances are modeled using "alpha-functions" (Rall 1967; Jack et al. 1975).

$$g_X(t) = \begin{cases} g_{max,X} \dfrac{t}{\tau_X} e^{1 - \frac{t}{\tau_X}}, & t \geq 0 \\ 0, & t < 0 \end{cases}, \quad X \in \{a, e, i\}. \qquad (5)$$

We also introduce the membrane time constant given by

$$\tau_m = g_m^{-1} C_m. \qquad (6)$$

Table 1 explains each model parameter and summarizes the values used for the different model parameters. In the majority of plots, we varied the maximum excitatory conductance (while other parameters were kept

constant). We set all parameters that were kept constant, to values found by Casti et al. (2008) to best describe the behavior of LGN neurons. The differential Eq. (4) was integrated using a first order Euler method with a time step of 0.1 ms.

2.5 Spike transfer ratio

Similar to Casti et al. (2008), we define the spike transfer ratio,

$$TFR = \frac{\#SPN \text{ spikes}}{\#DSRGC \text{ spikes}}, \qquad (7)$$

where "#" stands for "number of". According to Casti et al., the biological plausible *TFR* values of LGN-cells for input from (non-direction selective) RGCs is between 0.07 and 0.7 (with median 0.34, see Table 2 in Casti et al. 2008). Consequently, in our study, we imposed the constraint that *TFR* values of SPN spike train have to be in the above mentioned limits in order to be biologically plausible.

In our simulations, the *TFR* usually depends on stimulus direction φ_i and thus *DSi* and *iS* are often calculated from simulation runs with different *TFR*. For this reason, we use the maximum *TFR* value over all stimulus directions as the relevant parameter.

$$TFR = \max_i TFR(\varphi_i). \qquad (8)$$

2.6 Index of sharpening

To compare the direction selectivity of the output of the simulated postsynaptic neuron (SPN) with that of the driving neuron, we define the index of sharpening as

$$iS = \frac{DSi(SPN)}{DSi(DSRGC)}. \qquad (9)$$

Fig. 1 Simulation of a neuron postsynaptic to direction selective retinal ganglion cell (Transfer ratio for the presented data segment is 0.3). Upper plot shows spike sequence of a retinal direction selective ganglion cell that provides (excitatory) input to a simulated postsynaptic neuron. Middle plot describes time course of the membrane potential V_m of a SPN computed by integration of Eq. (4). Lower plot represents spike sequence of the SPN. Resulting firing events of the SPN (firing threshold is $V_{thresh} = -45$ mV)
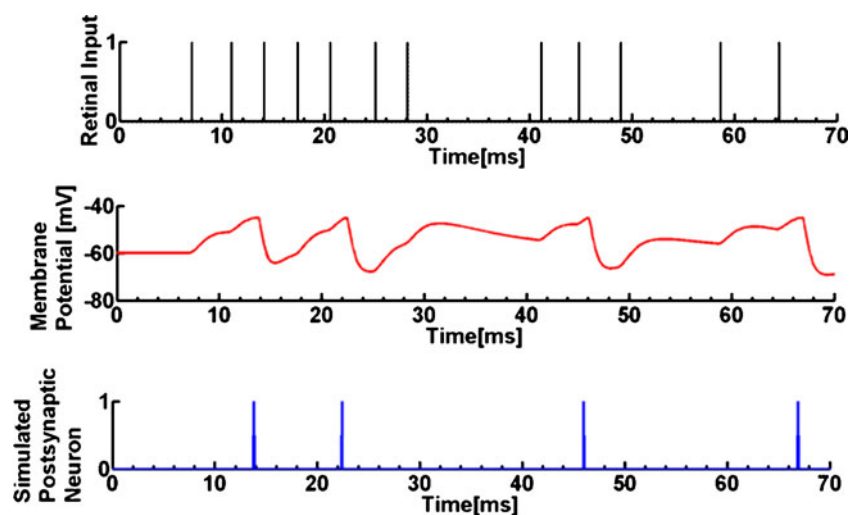
Table 1 Parameter values used in this study (for parameter that can have different values, the default value is highlighted in bold). The membrane conductance can be calculated from Eq. (6), $g_m = \tau_m^{-1} C_m$

Parameter	Value(s)
Membrane time constant τ_m	5 / 8 / **10** / 12 / 15 / 20 ms
Membrane capacitance C_m	1 nF
(Membrane conductance g_m	0.2 / 0.125 / **0.1** / 0.07 / 0.05 μS)
Resting potential V_{rest}	−60 mV
Threshold potential V_{thresh}	[−55 : −25] mV
Excitatory reversal potential E_e	20 mV
Inhibitory reversal potential E_i	−90 mV
Afterhypolarisation reversal potential E_a	−95 mV
Maximum excitatory conductance $g_{max,e}$	0.02 / 0.03 / 0.04/0.05 / 0.06/0.07 / 0.1 / 0.15 μS
Maximum inhibitory conductance $g_{max,i}$	**0** / 0.02 / 0.03 / 0.04 / 0.06 / 0.1 / 0.15 μS
Maximum afterhypolarisation conductance $g_{max,a}$	0.59 μS
Excitatory time constant τ_e	1 ms
Excitatory time constant τ_i	1 ms
Afterhypolarisation time constant τ_a	0.5 ms
Time delay for locked inhibition Δt_{ie}	1 ms

$iS > 1$ means that the SPN shows higher directional selectivity than the presynaptic neuron. For spike transfer ratios below 0.07, or above 0.7, we set iS to zero.

2.7 Artificial spike trains

In order to investigate which properties of spike trains effect sharpening, we also generated "artificial spike trains". These spike trains have the same average spike rates for different stimulus directions—and thus the same *DSi*—as spike trains recorded from DSRGCs. The firing probability was equally distributed over time according to a Poisson process except for defined refractory periods after each spike event. Spike trains with refractory period of 2 ms, 5 ms and 20 ms were generated.

3 Results

3.1 Sharpening of direction selectivity from ON-OFF direction selective cells

We first characterized the directional tuning of a simulated postsynaptic neuron (SPN) that receives input from a single direction selective retinal ganglion cell (DSRGCs). The spike trains of the DSRGCs have been recorded with a multi-electrode array. The SPN model adopted here incorporates several biophysical parameters that shape the spike transfer ratio: the passive membrane properties of the simulated postsynaptic neuron (SPN), (i.e. the membrane time constant), the synaptic conductance that determines the strength of PSPs and the spike threshold.

In a first simulation we varied the strength of synaptic excitatory conductance (parameter $g_{max,e}$). All other parameters were kept fixed (Table 1). Similar, biological plausible values have been reported by Wörgötter and Koch (1991) and Casti et al. (2008).

Figure 2(a) shows an example of the directional tuning of an ON-OFF DSRGC and its SPN counterpart for different $g_{max,e}$ values. This retinal cell had a preferred direction of 90°, and its DSi was 0.49. With excitatory synaptic input only, the SPN counterpart, is more directional selective than its retinal partner. The degree of sharpening—expressed as an index of sharpening (iS)—corresponds to the ratio of post- and presynaptic direction selective indexes, Eq. (9). We calculated iS values higher than 1 for a parameter range between $g_{max,e}$=0.06 μS (iS= 1.4) up to $g_{max,e}$=0.1(iS=1.2).

The degree of sharpening for ten ON-OFF direction selective neurons is shown in Fig. 2(b). For all simulated cells we obtain sharpening of directional selectivity up to a value of $g_{max,e}$ that leads to a transfer ratio of 0.7 ($g_{max,e}$=0.1 μS).

Weak synaptic inputs (i.e. $g_{max,e} < 0.04$ μS) did not lead to sharpening in direction selectivity, because most of the spikes were not transmitted any more across the synapse (transfer ratio, Eqs. (7) and (8) below 0.07). As the strength of excitatory synaptic input grew, for four (out of ten) cells iS exceeded 1 already at $g_{max,e}$=0.04 μS (Fig. 2(b)). Excitatory synaptic inputs with $g_{max,e} \geq 0.05$ μS always led to iS>1. The mean value of iS=1.30 (std=0.20, n=10) at $g_{max,e}$=0.05 μS, slightly decreased to iS=1.11 (std=0.06, n=10) at $g_{max,e}$=0.1 μS. For a strong synapse ($g_{max,e}$= 0.12 μS) the transfer ratio (TFR) exceeds the maximum value of 0.7. At this value almost every EPSP is capable of evoking an action potential at the SPN. Thus the DSi of the
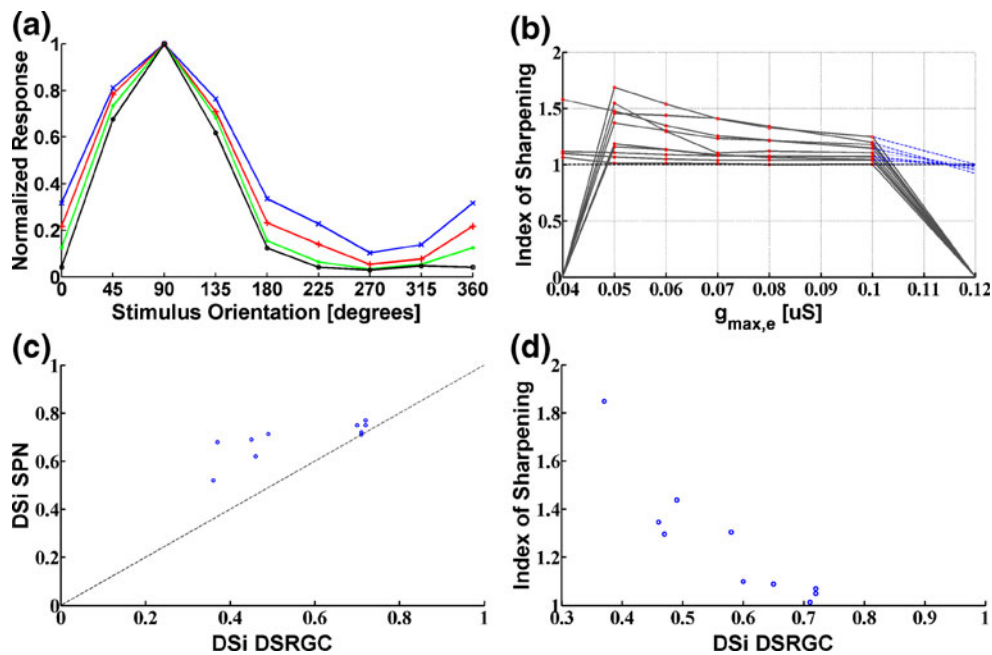
Fig. 2 The directional tuning of model neurons increases if ON-OFF direction selective cells provide monosynaptic input. Index of Sharpening iS = DSi(SPN)/DSi(DSRGC), Eq. (9). Red dots indicate the values for which transfer ratio was between the considered limits of 0.07–0.7 (**a**) Normalized (mean) responses (averaged over 7 trials) of an ON-OFF (*blue curve*) and of SPNs receiving excitatory input from the DSRGC for different synaptic conductances $g_{max,e}$. While the DSRGC has direction selectivity index DSi=0.49, the simulated neurons have higher DSi values and thus iS>1: For $g_{max,e}$=0.1 μS (*red curve*) we have DSi=0.59 resulting in iS=1.2. For $g_{max,e}$=0.08 μS (*green curve*), we have DSi=0.66 and iS=1.34, for $g_{max,e}$=0.06 μS (*black curve*) DSi=0.72 and iS=1.4 (**b**) Index of sharpening (iS) computed for 10 ON-OFF DSRGCs and their simulated postsynaptic counterparts for different

maximum excitatory conductance $g_{max,e}$ (*gray curves*). On the average, we find sharpening (iS>1) for $g_{max,e} \geq 0.04$ μS up to 0.1 μS. For $g_{max,e} \geq 0.12$ μS no significant sharpening is observed (DSi(SPN) ≈ DSi (DSRGC), iS≈1) because each input spike triggers an output spike in the simulated postsynaptic neuron for high synaptic conductances, see *blue dashed lines*. For DSRGCs with high DSi, maximum iS = DSi (SPN)/DSi(DSRGC) is usually lower than for DSRGCs with low DSi. (**c**) Direction selectivity index for postsynaptic model neuron is higher than direction selectivity index of ON-OFF DSRGCs (for all cells). For this figure $g_{max,e}$=0.06 μS. (**d**) The degree of sharpening depends on presynaptic direction selectivity. The higher the DSi of presynaptic cell the lower the iS at SPN

SPN approaches the DSi of presynaptic cell resulting in iS≈ 1. This is shown by blue dashed lines in Fig. 2(b) which point out that iS stays close to 1 if TFR was ignored. Mean iS (at $g_{max,e}$=0.12 μS without taking into consideration TFR)=0.97(std=0.02, n=10).
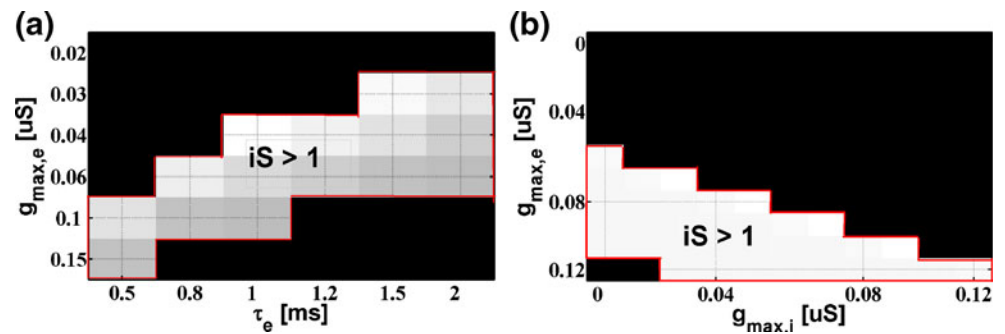
The degree of sharpening depends also on the tuning of the presynaptic cell. For an excitatory synapse of $g_{max,e}$=0.06 μS, the iS decreases for increasing direction selectivity indices of the retinal driver as indicated in Fig. 2(c). For ON-OFF DSRGCs with low DSi, sharpening at the postsynaptic neuron is stronger than that observed for high presynaptic DSi. Figure 2(d) illustrates the finding that less sharpening is obtained if the retinal ganglion cell itself is highly tuned. In conclusion, sharpening in directional selectivity was achieved for all tested ON-OFF DSRGCs and was more prominent for presynaptic inputs with a lower DSi.

In a next set of simulations, we investigate how robust sharpening is, with respect to variations (of postsynaptic parameter) of the EPSPs' time constant (Fig. 3(a)) and the introduction of an additional inhibitory conductance (Fig. 3(b)).

We varied the EPSP's time constant and analyzed the additional effect that this parameter has on the iS. As EPSP time constant increases we found that sharpening is achieved at low $g_{max,e}$ values (Fig. 3(a), red contour indicates the areas where sharpening at postsynaptic target was achieved). For a constant strength of excitatory conductance we always find that sharpening is reduced as time constant of EPSP is increasing. This finding is simply explained by the fact that if the EPSP is prolonged the temporal summation of EPSPs will give rise to a large number of spikes at SPN and thus to a lower iS. By contrary, at low τ_e values, sharpening is achieved for strong excitatory synaptic input only.

A stimulus that is larger than the center of the receptive field could provoke additional inputs from neighboring retinal cells directly or by mean of local interneurons (Alitto and Usrey 2005; Carandini et al. 2007). To investigate the effect of such a situation we added, in addition to excitatory input, inhibitory synaptic input convergent on the same postsynaptic model neuron. For the inhibitory conductance we used a fixed time delay of 1 ms with respect to the

Fig. 3 Index of sharpening for a postsynaptic model neuron that receives input from a ON-OFF DSRGC in dependence on maximum excitatory conductance $g_{max,e}$ and EPSP time constant τ_e (**a**) or maximum inhibitory conductance $g_{max,i}$ (**b**). The red contour line highlights areas where TFR is within the range [0.07, 0.7] and index of sharpening is higher than 1

excitatory inputs. Both, excitatory and inhibitory synaptic inputs are sent by the same DSRGC. Time locked excitation and inhibition has been found in the retinogeniculate pathway (Blitz and Regehr 2005). Variation of these parameters under the transfer ratio restriction (i.e. 0.07≤ TFR≤0.7) demonstrates that over a wide range of model parameters the postsynaptic neuron has a higher index of direction selectivity than its presynaptic main driver.

As expected, if $g_{max,i}$ increased (strong inhibition) $g_{max,e}$ must also increase in order to achieve sharpening at SPN. Thus, if $g_{max,e}$ takes low values ($g_{max,e}<0.05$ μS, Fig. 3(b)) no sharpening at the postsynaptic level can be obtained.

Altogether, the scenarios presented so far suggest that direct monosynaptic excitatory input is sufficient to achieve sharpening at postsynaptic neuron for a wide range of biologically plausible synaptic strengths. Additional parameters, describing postsynaptic neuron properties or involving polysynaptic mechanism, do not radically change the sharpening in direction selectivity at the SPN.

3.2 Sharpening of direction selectivity from ON direction selective cells

In addition to the ON-OFF direction selective neurons, we investigated a second type of direction selective cells—the ON DS cells. These cells have broader directional tuning and thus smaller DS indices than ON-OFF DS cells.

In contrast to the extensive sharpening of small DS indices from ON-OFF cells (Fig. 2(c)) we find little sharpening for the three ON DS cells investigated (Fig. 4(a)). The simulations were performed analogous to the ON-OFF DS cells with the constraint on the transfer ratio. For one of the cells we found sharpening at SPN only for a single $g_{max,e}$ value (Fig. 4(a), $g_{max,e}=0.1$ μS, iS= 1.1) while the other two cells presented iS higher than 1 for a restricted range of $g_{max,e}$ values ($g_{max,e}\geq0.07$ μS and $g_{max,e}\leq$ 0.1 μS for one cell and $g_{max,e}\geq0.06$ μS and $g_{max,e}\leq0.1$ μS for the other cell). The degree of sharpening is less pronounced than in the case of ON-OFF DSRGCs and in mean it starts exceed 1 only at $g_{max,e}=0.07$ μS when iS= 1.11. Beyond $g_{max,e}=0.1$ μS no sharpening is achieved due

to the fact that such strong synaptic input is generating almost at each EPSP an AP at SPN so that iS tends to be almost 1 (as indicated by the blue curve in Fig. 4(a) if TFR were ignored). Thus, for ON DS RGCs we found less sharpening when comparing with ON-OFF DSRGCs in the same simulation conditions.

3.3 Sharpening of directional selectivity from artificial spike trains mimicking direction selective neurons

Apparently, the presynaptic degree of directional tuning does not provide evidence how the sharpening works. We therefore considered artificial spike trains that mimicked the firing rate and thus directional tuning of ON-OFF as well as ON DS cells. The spike trains followed a Poisson distribution. We calculated the postsynaptic sharpening for a total of ten artificial spike trains. Each spike train mimicked the directional tuning of the ten recorded ON-OFF DS. Additionally, we built artificial spike trains with similar index of selectivity as one ON DS cell having DSi= 0.34. For each of the firing rates we consider three refractory periods: 2 ms, 5 ms and 20 ms.

Among the artificial spike trains, both, sharpening obtained for the widest gmaxe range and the highest iS values are found for short ISIs (i.e. refractory period of 2 ms). For spike trains with short refractory periods (minimum 2 ms) the sharpening at SPN, for all ten simulated spike trains, is achieved for an interval of $g_{max,e}=[0.07–0.1]$ μS (Fig. 4(b), red curve) more restricted than for the real ON-OFF DSRGCs for which we found sharpening for a larger interval $g_{max,e}=[0.05–0.1]$ μS (Fig. 2(b)). For these artificial spike trains, at $g_{max,e}=$ 0.06 μS mean iS=0.53 (std=0.69, $n=10$), while at $g_{max,e}=$ 0.06 μS the recorded ON-OFF DSRGCs show a much higher mean index of sharpening, iS=1.30. The best sharpening for all ten artificial spike trains has its mean iS value iS=1.39 (std=0.22, $n=10$). For the ten recorded spike trains the maximum value of sharpening is higher, iS=1.41(std=0.23, $n=10$).

Increasing the refractory period to 5 ms we found, the mean, sharpening for a more restricted interval of $g_{max,e}=$ [0.08–0.1] μS (Fig. 4(c), red curve). Mean iS indicates the
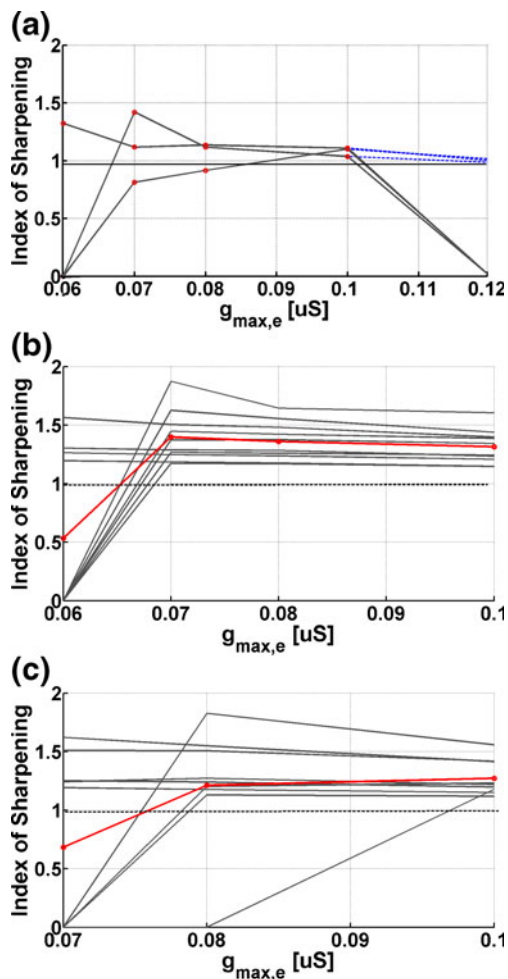
Fig. 4 Index of sharpening for ON DS and artificial spike trains (**a**) Index of sharpening for 3 ON DSRGCs . For ON-DSRGCs, sharpening is obtained only for conductances larger $g_{max,e} \geq 0.07$ μS. Red dots in the plots indicate $g_{max,e}$ values for which TFR is in the validation domain, while blue dashed lines indicate the iS value if TFR were ignored. (**b**) Index of sharpening for 10 artificial spike trains mimicking the 10 ON-OFF DSRGCs recorded and post-synaptic model counterparts. Refractory period is 2 ms. Mean iS (*red curve*) is indicating a sharpening for a more restricted $g_{max,e}$ interval than for recorded cells (Fig. 2(b)) regardless the fact that they have similar firing rates and DSi. Best sharpening among artificial spike trains, is obtained for 2 ms refractory period spike trains and is less present as refractory period increase. At 20 ms iS>1 only at $g_{max,e}$= 0.1 μS. For ON DSRGC we found iS>1 only for a single $g_{max,e}$ value=0.1 μS. (**c**) Index of sharpening for 10 artificial spike trains mimicking the 10 ON-OFF DSRGCs recorded with a refractory period of 5 ms. For these artificial spike trains the sharpening at SPN is even more restricted

highest sharpening for these artificial spike trains at $g_{max,e}$= 0.08 μS, mean iS=1.21 (std=0.47, n=10). Thus for longer refractory periods, the sharpening achieved is also more restricted compared to recorded ON-OFF DSRGCs.

For the spike trains with 20 ms refractory period we found sharpening only for $g_{max,e}$=0.1 μS(data not shown here). For

the artificial spike trains mimicking ON DS cell we achieved sharpening only at $g_{max,e}$=0.1 μS and only if the refractory period was set at 2 ms (data not shown here).

If firing rates of the presynaptic cell would be responsible for sharpening at postsynaptic neuron, subsequently one would expect similar iS (for similar $g_{max,e}$ values) to be obtained at the output of artificial spike trains with the same DSi as the recorded cells. Instead, we found a more restricted parameter range for which sharpening can be achieved for the artificial spike trains.

3.4 Burst-like spiking activity carries
the directional-selective information

The results from the artificial spike trains indicate that sharpening of directional tuning does depend on the short inter spike intervals encountered in some direction selective cells. It does not depend on the neuron's firing rate that is different for the different recorded DSRGCs and artificial spike trains (compare Figs. 2(b) and 4). We therefore investigated the intrinsic spike train properties of DSRGCs. We selected a parameter often used in the analysis of LGN neurons: the percentage of bursting. Burst-like events were identified and quantified as described in Methods (Section 2.3). We calculated the burst-rate in the response of ON-OFF DS cells as well as ON DS and artificial Poisson-like spike trains.

We found that burst-like activity was more pronounced for the ON-OFF DSRCs than for the ONDS cells or for the artificial spike trains. As shown in Fig. 5(a) burst rate at preferred direction for ON-OFF cells was highest, the mean for all ten cells was 2.29 +/− 0.9(n=10) [bursts/sec], even ten times higher than for ONDS cells for which mean burst rate for all trials was only 0.07 +/− 0.06(n=3) [bursts/sec]. For artificial spike trains we also found a lower burst rate at preferred direction even though the firing rate mimicked that of the ten recorded ON-OFF DSRGCs. While for spike trains with 2 ms refractory period we could find a sharpening more pronounced than for the spike trains with refractory period of 5 ms and 20 ms, we also found a burst rate at preferred direction higher for these spike trains with a mean of 0.54 +/− 0.15 [bursts/sec], (n=10). As in Fig. 5 (a), once that refractory period increased the artificial spike trains diminished their burst-like activity, so that we found for 5 ms refractory period a mean burst rate of 0.04 +/− 0.04 [bursts/sec], (n=10), and for 20 ms refractory period 0.03 +/− 0.02 [bursts/sec], (n=10).

Beside this discrepancy there are two more factors that worth to be noted −one is that burst-like activity for ON-OFF DSRCs was tuned at preferred direction (Fig. 5(c) show the tuning curves for one ON-OFF DSRGC calculated from firing rate (blue) and burst rate (green)— the preferred direction indicated by maximal firing rate
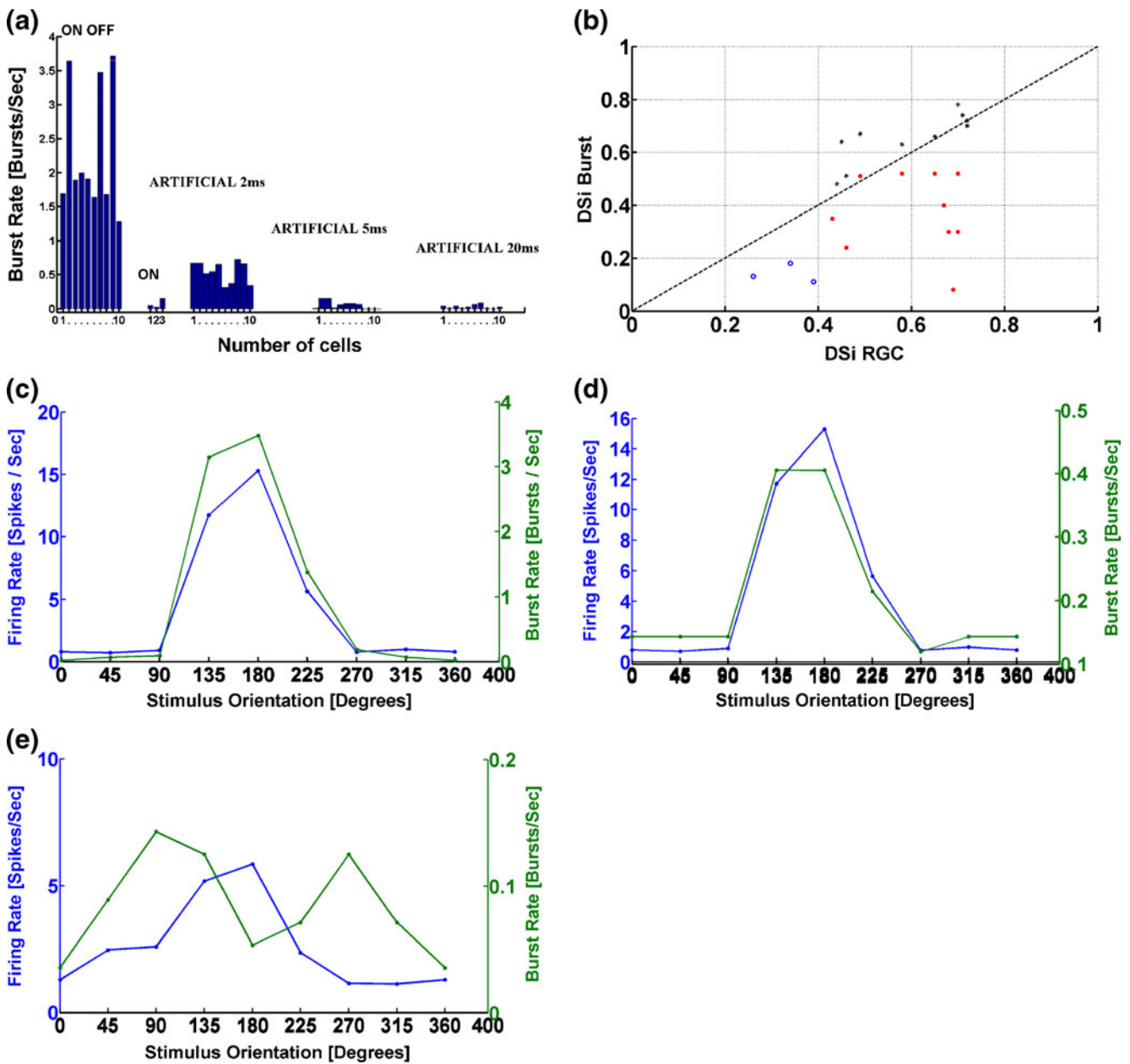
Fig. 5 Burst-like activity (**a**) Burst rates at preferred direction calculated for recorded cells and for artificial spike trains. The highest burst-like activity is obtained for ON-OFF DSRGCs. ON DS cells show almost no burst-like activity. Artificial spike trains also exhibit reduced burst-like activity. X axis indicate the number of cells for which the burst rate at preferred direction was quantified. (**b**) Index of selectivity for burst-like events (Y axis) and for firing rate (X axis) shows that only for ON-OFF DSRGCs (*dark dots*) DSi Burst is higher than DSi firing rate. For ON DS cells (*blue dots*) and for artificial spike trains (with 2 ms refractory period) DSi Burst is lower than DSi firing rate. (**c**) Tuning curves of firing rate (*blue curve*) and burst rate (*green curve*) for one ON-OFF DSRGC. Burst rate is more sharpened (DSi=0.78) than firing rate (DSi=0.70) and oriented at preferred direction. (**d**) Tuning curves of firing rate (*blue curve*) and burst rate (*green curve*) for one artificial spike train that mimics the ON-OFF DSRGC presented in Fig. (**a**). In this case DSi^{burst} (DSi=0.30) is considerable lower than DSi firing rate (DSi=0.70) and does not singularly indicate the preferred direction. (**e**) Tuning curves of firing rate (*blue curve*) and burst rate (*green curve*) for one ON DS cell. Burst-like activity is clearly not pointing the preferred direction and it's DSi^{burst} (= 0.11) is lower than DSi firing rate (= 0.39)

coincides with the preferred direction calculated from burst rate). That is, at preferred direction ON-OFF DSRGCs show burst-like activity more than at intermediate directions. In this way the probability of evoking an AP at SPN becomes higher at preferred direction while

two (or more) closed (in time) EPSPs are more successful in rising membrane potential of SPN above the threshold. This phenomenon is known as paired spike enhancement and has been demonstrated at many synapses (Usrey et al. 1998; Carandini et al. 2007). The burst rate for ON DS

cells and artificial spike trains was almost equal zero and pointing non-preferred directions (Fig. 5(d, e)).

We used burst rate for each presentation direction to calculate the degree of directional selectivity. Once we calculated the burst rate at each direction of stimulus presentation we next used DSi^{burst} as described by Eq. (2), in a manner similar to that used for firing rate, and we calculate the direction selectivity index for burst-like spiking.

The other important factor is that tuning curves for burst rate were more sharpened than the tuning curves of firing rates for ON-OFF DSRGCs, so that the index of selectivity for burst-like activity (DSi^{burst}) was always higher than DSi firing rate (black dots Fig. 5(b)). By contrary DSi^{burst} for ONDS cells (Fig. 5(b) blue dots) and for artificial spike trains with 2 ms refractory period (Fig. 5(b) red dots) was lower than DSi calculated from firing rates.

In summary, for the ten ON-OFF DSRGCs we found a mean burst rate at preferred direction significantly higher than for ON DS cells or artificial spike trains. Burst-like activity is tuned at preferred direction and has a higher DSi than firing rate for ON-OFF DSRGCs as compared with ON DS or artificial spike trains which show the opposite results.

It is already well known that these two different RGC types posses different spike train signatures (Zeck and Masland 2007). Our analysis shows also that ON-OFF cell type exhibit burst-like activity at preferred direction while ON cell type has less or no burst-like activity.

That short ISIs in the presynaptic spike trains are recognized to be very important in transmitting information at different stages within the brain is already well known (Sincich et al. 2007; Rathbun et al. 2007). In our example burst-like activity seems to be the key in signaling better the direction of motion of visual stimulus at the output of retina.

We went further into more detailed analysis and calculated the number of postsynaptic APs due to presynaptic burst-like firing. We scanned the spike trains of both, presynaptic and postsynaptic cells, and counted the spikes at SPN due to burst-like activity in presynaptic spike train for each pair of pre- and post-synaptic cells. In this manner we could quantify the efficacy and influence of the presynaptic burst-like activity (B^e) as the number of spikes at SPN due to bursts at preferred direction divided by the total number of spikes at SPN, at preferred direction, for each pair of cells (Eq. 3).

For the ten recorded ON-OFF DSRGCs we found that mean B^e has its maximum at the best sharpening observed. Remarkably, once that $g_{max,e}$ increases, mean TFR also increases, while both, mean B^e and iS decrease (Figs. 6(a) and 2(b)). This is explained by the fact that at low $g_{max,e}$ the number of postsynaptic spikes, at preferred direction, due to burst-like activity of the presynaptic cell is the highest compared with the total number of spikes at SPN, at

preferred direction. At this point the best sharpening is observed. Once $g_{max,e}$ increases, the number of spikes at SPN increases, but the number of spikes at SPN due to a burst in presynaptic cell decreases and we notice a less pronounced sharpening. While for the best observed sharpening, B^e has a maximum, for less sharpening the number of spikes at non-preferred direction increases and the influence of the burst-like activity of the presynaptic cell is diminished. It is crucial to point out that these findings bring us to the following remark—burst-like spiking activity is carrying the information about direction selectivity. Thus, at best sharpening this component of the spike train that can inform about direction of stimulus movement at preferred direction is preserved (B^e has its maximum) while the components signaling the movement of stimulus at intermediate directions are lost.

The mean B^e for the ON-OFF DSRGCs was at its maximum 0.45 +/− 0.25 ($n=10$) and it decreased to 0.36 +/− 0.18 ($n=10$) at its minimum.

For the artificial spike trains with 2 ms refractory period mean B^e at its maximum was only 0.12 +/− 0.06 ($n=6$) and decreased at 0.06 +/− 0.03 ($n=6$) at its minimum (Fig. 6(b)).

Once we calculated the number of spikes at SPN due to burst-like activity at presynaptic cell for each pair of cells, we then calculated (in the same manner as for firing rates) the indexes of selectivity of these SPN spikes, due to bursts ($DSi\ SPN^{burst}$). Figure 6(c) shows that for the ON-OFF DSRGCs, mean $DSi\ SPN^{burst}$ is always higher than DSi SPN and is decreasing as $g_{max,e}$ increases and sharpening decreases. This means that if the spike trains at SPN were only due to burst activity in the presynaptic cells we were having a higher degree of sharpening. Due to the fact that the TFR is increasing with $g_{max,e}$, the increasing number of APs at non-preferred directions is lowering the degree of sharpening. However, $DSi\ SPN^{burst}$ always remains higher than DSi SPN and indicates the burst events control the degree of sharpening.

For the artificial spike trains (Fig. 6(d)) the effects are different. Firstly, we always observed that DSi at SPN is higher than $DSi\ SPN^{burst}$, so that the number of spikes due to bursts is not able to control the sharpening at SPN. Moreover, even if $DSi\ SPN^{burst}$ is increasing as $g_{max,e}$ increases (opposed as in ON-OFF DSRGCs case), the degree of sharpening is decreasing (DSi SPN decreases). This strengthens the fact that burst-like activity for artificial spike trains (substantially less present than for ON-OFF DSRGCs) does not control the sharpening at SPN.

For two of the ONDS cells we did not find any spike at the SPN, at preferred direction, due to burst-like activity at the presynaptic level. For the third ONDS cell we found at SPN level a few spikes due to burst-like activity at the presynaptic level. In this case (Fig. 6(e, f)) we found
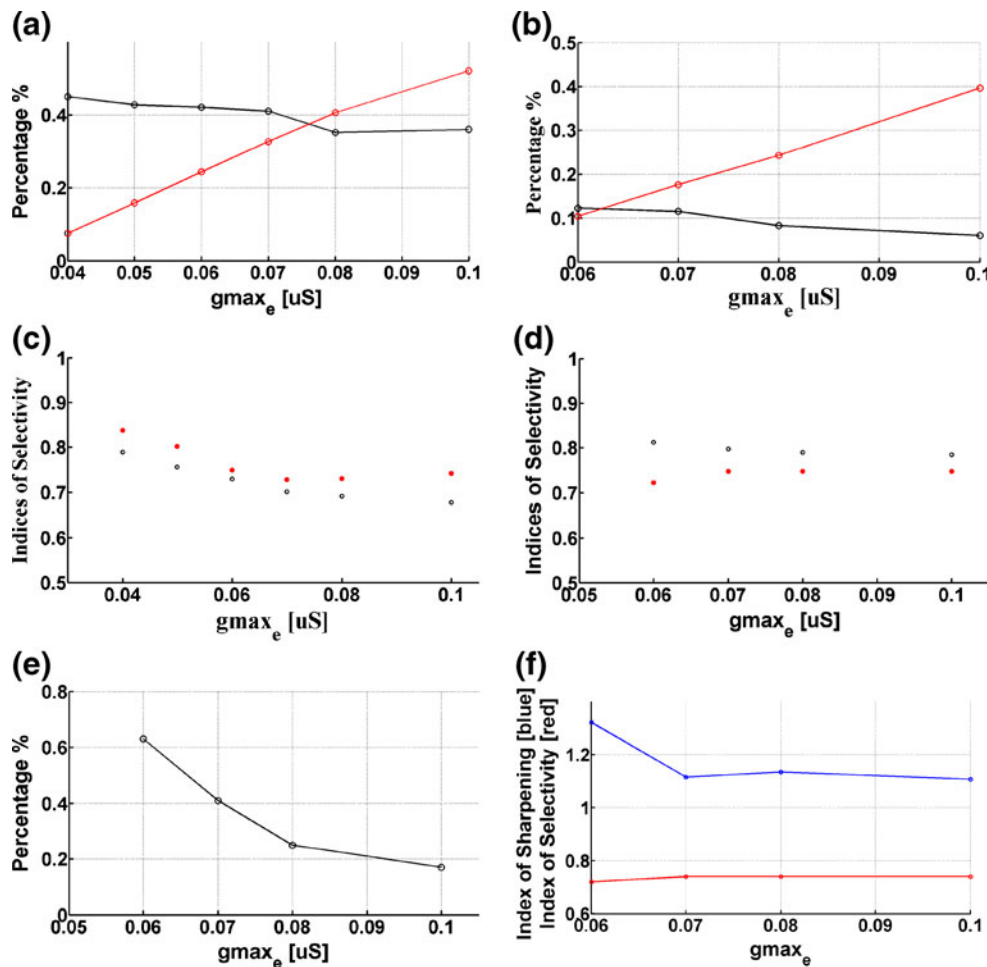
Fig. 6 Burst efficacy and index of sharpening (**a**) Black dots represent mean burst efficacy (B^e) as described by Eq. (3), for 10 ON-OFF DSRGCs. Red dots show the TFR course as g$_{max,e}$ increases. B^e is decreasing as TFR increases due to a larger number of spikes at intermediate direction, as a consequence iS is decreasing too (see Fig. 2(b)). (**b**) Black plot is mean burst efficacy and red dot is mean transfer ratio. For the artificial spike trains that mimic the 10 recorded ON-OFF DSRCs B^e is lower than for the recorded cells and also decreases as TFR increases. (**c**) DSi at SPN due to burst-like activity measured for 10 ON-OFF DSRCs (*red dots*) is higher than DSi at SPN (*black dots*) and is controlling the sharpening at SPN. As g$_{max,e}$ increases DSi at SPN due to burst-like activity is decreasing and as a consequence iS is also decreasing. (**d**) For the artificial spike trains that

mimic the recorded cells DSi at SPN due to burst-like activity (*red dots*) is permanently lower than DSi SPN (*black dots*) and is increasing as iS decreases, hence proving no control mechanism over the sharpening at SPN. (**e**) One single ON DS cell presented spikes at SPN due to burst-like activity at the presynaptic level. This cell has B^e (*black dots*) with a drop as g$_{max,e}$ increases. (**f**) Index of sharpening (*blue dots*) and index of selectivity (*red dots*) for the same ON DS cell as above. Interestingly, as g$_{max,e\ increases}$ from 0.06 to 0.07, DSi increases while iS decreases. Moreover Fig. (e)) shows that as g$_{max,e}$ increases from 0.07 to 0.08, B^e decreases but contradictory iS increases (*blue dots*) showing that there is no direct mechanism based on burst-like activity to enhance sharpening (iS) for ON DS cell

that while B^e decreases from g$_{max,e}$=0.07 to 0.08, the index of sharpening is slightly increasing, for the same parameter values (Fig. 6,(f) -blue dots). Additionally, DSi^{burst} increases for g$_{max,e}$=0.06–0.07 (Fig. 6,(f) -red dots) while index of sharpening is decreasing for the same values of g$_{max,e}$ (Fig. 6,(f) -blue dots) . Altogether with the fact that DSi^{burst} was always lower than DSi SPN and the very low burst rate that we found, led us to the conclusion that burst-like activity is not at the origin of sharpening we found for ONDS cell, indeed for a more restricted parameter range than for the ON-OFF DSRGCs.

3.5 How is the enhancement performed at the postsynaptic cell?

So far we have found that burst-like activity carries the information about direction of stimulus movement. This intrinsic property is commonly found at ON-OFF DSRGCs and is predominant at preferred direction of stimulus movement. It has been already shown that PSP summation and spike threshold suffice to explain the transformation of the retinal input spike train to a new spike train output of LGN cell. In our simulation conditions, summation of the
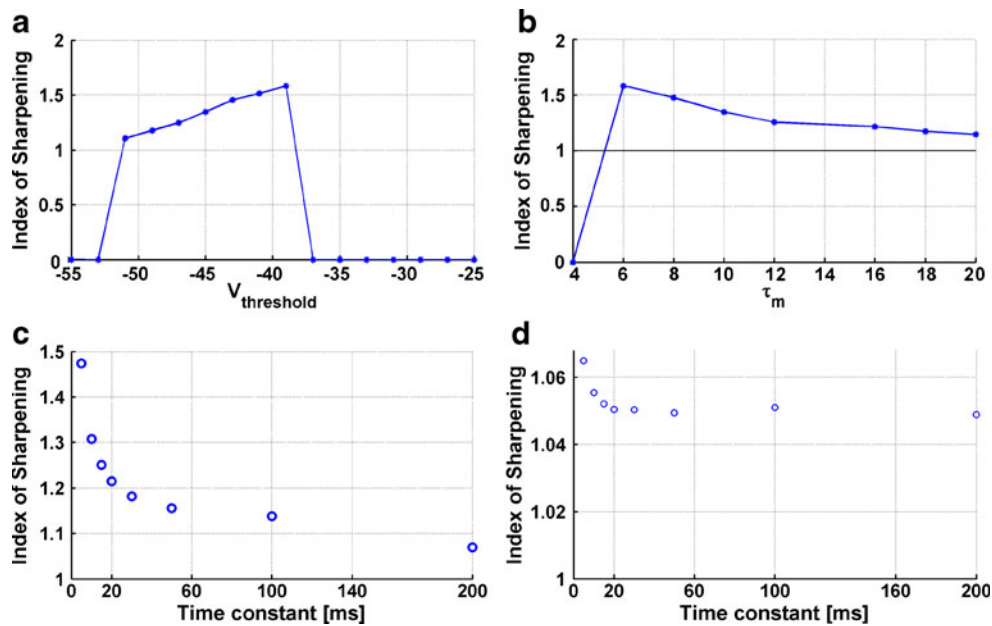
Fig. 7 Model enhancement mechanism (**a**) Relation between iS and $V_{threshold}$ for a typical input spike train of an ON-OFF DSRGC with DSi=0.49. As spiking threshold increases the sharpening obtained is larger due to the fact that only at preferred direction EPSPs summation can raise the membrane potential above the threshold. However, for large thresholds there are only a few APs evoked at the SPN, so that iS=0. (**b**) Cell's membrane time constant variation is depicted on X axis. Best sharpening is at low time constant values. Indeed for low τ_m values, the EPSPs are closed enough in time, in order to realize the temporal summation, only at preferred direction during the burst-like spiking activity. (**c**) Nonlinear amplifier with a specific time constant (X axis) applied to an incoming retinal spike train with a middle DSi= 0.49. Index of sharpening (Y axis) decreases as time constant increases. (**d**) Nonlinear amplifier with a specific time constant (X axis) applied to an incoming retinal spike train with a very high DSi= 0.72. The temporal filter gives a sharpening for τ_m=5 ms, almost as good as for τ_m=200 ms. The influence of the temporal filter is reduced comparing with low tuned presynaptic cell

incoming retinal EPSPs combined with postsynaptic spike threshold act as a temporal filter to perform a selective reduction in gain for long ISI presynaptic discharge and to increase in gain for short ISI spike trains.

To see more in details how this filter works, we checked firstly the relation between spike threshold membrane potential ($V_{threshold}$) at the SPN and index of sharpening for a typical input of ON-OFF DSRGC and middle value of $g_{max,e}$=0.06 µS (Fig. 7(a)). We varied $V_{threshold}$ from −55 mV up to −25 mV. As $V_{threshold}$ increased iS also increased, so that at −51 mV we found iS= 1.1 and at $V_{threshold}$=−39 mV iS increased at iS=1.58.

This is explained very simple. Once that $V_{threshold}$ increased, at $g_{max,e}$ constant, it is necessary to have more closed in time EPSPs to rise the membrane potential above the threshold value, that is, a pronounced burst-like activity (short ISI) in the DSRGC spike train. At the intermediary directions of stimulus movement, burst-like activity (short ISI) is lower than at the preferred directions for ON-OFF DSRGCs (Fig. 5(c)) and thus the summation of EPSPs become less efficient as $V_{threshold}$ increases. The result is that for intermediary directions less APs at SPN will be evoked so that the information about these directions of stimulus movement will be lost. By contrary, at preferred directions, burst-like activity (short ISI) is more accentuated, and will be sufficient amount of closed EPSPs to sum and raise the membrane potential above the threshold to produce APs at SPN. Thus, this component of the input spike train, signaling the preferred direction, will be preserved. As expected, if $V_{threshold}$ continue to further increase, at some value, too little amount of APs at SPN will be evoked so that TFR will be below its limit and iS becomes zero (Fig. 7(a)).

Furthermore, we checked the relations between cell's time constant (τ_m) and iS for a middle value of V_{thresh}=−45 mV and a middle value of $g_{max,e}$=0.06 µS (Fig. 7(b)). At τ_m=6 ms, iS=1.58, while at τ_m=20 ms we found iS=1.14. For a low τ_m value, if the ISi is large (slow input spike train) EPSPs do not sum together to force the membrane potential to reach the threshold. Thus, at preferred directions, where the ISI is shorter, the chance to have APs at SPN is greater and thus iS is higher. Once that τ_m increases, the ISI necessary for temporal summation to take place increases also, so that at intermediary directions the chances to have APs at SPN increases too, resulting in a decrease of iS (Fig. 7(b)).

To have a better intuition over the temporal filter that acts upon the incoming retinal input we built a simpler mathematical model which depicts a nonlinear amplifier

with a specific time constant and applied it over the inverse spike intervals of a typical input spike train (Fig. 7(c)). Briefly, we calculated the ISI for a typical recorded spike train of one ON-OFF DSRGC (DSi=0.49). We established two thresholds, the low limit representing the refractory period and high limit representing the specific time constant (τ). Once that ISI is higher than the low limit and lower than the high limit, we hypothesized that PSPs summation was possible and we counted an AP at the SPN. We then calculated the tuning curve of the SPN and thus the index of sharpening. At low values of time constant τ=5 ms we found the best sharpening iS=1.47. As τ increased the sharpening decreased, so that at τ=200 ms we found iS= 1.06. Therefore, if τ<5 ms we found best sharpening and indicates the fact that most of the short ISI (ISI<5 ms) spiking activity is encountered at preferred direction strengthening the probability that closed EPSPs to sum and evoke APs at SPN. As τ increase sharpening becomes weaker indicating that large ISI spiking activity is often found at intermediate directions of stimulus movement, so that when cell's time constant becomes larger, temporal summation of EPSPs will evoke APs at intermediate directions too, decreasing iS.

We also have shown that the degree of sharpening depends on the tuning of the presynaptic cell so that for input spike trains with high DSi the index of sharpening obtained was lower than for input spike trains with low DSi (Fig. 2(d)). This simpler mathematical model which shows the ISI distribution explains why iS is low for high presynaptic DSi. Briefly, for a recorded spike train of one ON-OFF DSRGC with high DSi (DSi= 0.72) we found a sharpening iS=1.06 at τ=5 ms and iS=1.04 at τ=200 ms (Fig. 7(d)). Therefore, even that time constant varied with almost 200 ms the sharpening suffered only a slight change. The result indicates that for cells with very high DSi the distribution of short ISI is highly concentrated at preferred direction. The temporal filter which acts upon the input spike train and enhances the sharpening has a lower effect in this case, while long ISI spiking activity (component which is lost for cells with lower DSi in order to enhance the sharpening) is less present. Comparing Fig. 7(c) and (d) one can observe the difference in the influence of the temporal filter and spike threshold over the index of sharpening. We found for low tuned ON-OFF DSRGC a decrease in iS of about 1.42 since for highly tuned presynaptic cell the decrease of iS was only 1.01, and thus iS remaining almost the same.

3.6 Polysynaptic directional selective input onto one model neuron

So far we considered monosynaptic connections of different pairs each consisting in one recorded DSRGC and one model neuron. It is assumed that several retinal cells can converge on the same postsynaptic target (Blitz and Regehr 2005; Sincich et al. 2007; Usrey et al. 1998). In the following we consider the hypothetical case of polysynaptic input with equal weights from several DSRGCs to a model postsynaptic neuron. In this hypothetical case of polysyn-aptic input we aligned the spike trains of the two convergent inputs according to the peak measured in their spike trains cross- correlogram. We asked what the effect is over the sharpening at SPN of simultaneous convergent synaptic inputs from two ON-OFF DSRGCs with the same preferred directions compared with the scenario of two ON-OFF DSRGCs having opposed preferred direction.

We recorded two ON-OFF DSRGCs in the same retinal portion responding preferentially to the same direction of stimulus movement (90° preferred direction). In a second recording portion we recorded another pair of ON-OFF DSRGC with opposed preferred direction (180° and 0° respectively). We calculated cross correlation histograms (CCH) for these pairs of neurons simultaneously recorded. We found a correlated activity with a time lag in CCH of 2 ms for which a maximum correlation between their spike trains was achieved. Further on we aligned the spike trains of formed pairs, extracting the peak observed in the CCH, in order to build simultaneous synaptic inputs to the same postsynaptic neuron.

Firstly, we found that the effect of hypothetical simul-taneous polysynaptic input consisted in shifting the range of the values for $g_{max,e}$ at which sharpening in direction selectivity was achieved. This shift was toward lower $g_{max,e}$ values. As expected, if two simultaneous excitatory synaptic inputs converge on the same postsynaptic target, then the strength of the synaptic conductances must not be too high. At low values of $g_{max,e}$ (even less than 0.03 μS) already the maximum sharpening is achieved for polysynaptic mecha-nism. When $g_{max,e}$ is increased, the number of APs at SPN increased also and for relatively high values of $g_{max,e}$ (>0.07 μS) the transfer ratio is already exceeding the maximum limit of 0.7 for most of the polysynaptic mechanism SPN and thus iS becomes zero (Fig. 8(a)).

Another important remark comparing Fig. 8(a) and (b) is that for the case of two simultaneous convergent inputs of ON-OFF DSRGCs with opposed directions the sharpening obtained at SPN is considerably reduced than iS for the scenario of two convergent inputs with the same preferred directions, and thus information regarding direction of stimulus motion will be at least not enhanced if not diminished at the postsynaptic level.

4 Discussion

The complexity of synaptic connectivity from retina to higher brain areas has been extensively studied (Kara and Reid 2003; Levick et al. 1969; Usrey et al. 1998).
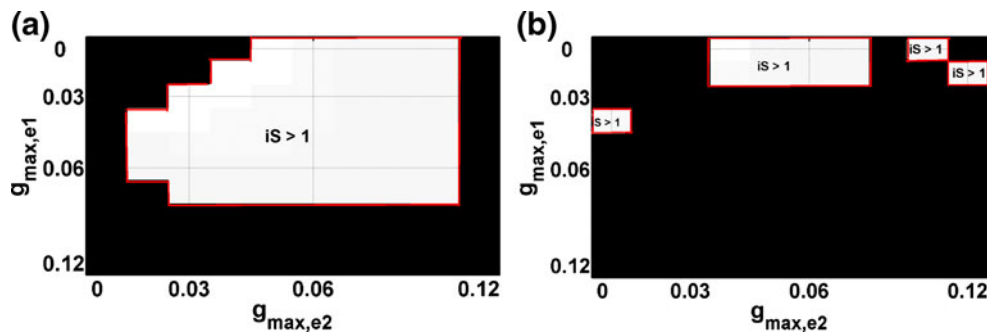
Fig. 8 Polysynaptic connectivity (**a**) Index of sharpening at SPN for the case of two different ON-OFF DSRGCs which send simultaneous convergent inputs to the postsynaptic cell. Presynaptic cells have different indices of selectivity, DSi1=0.59 and DSi2=0.72. The two cells have the same preferred direction at 90°. Index of sharpening at SPN is calculated as DSi SPN / DSi2 DSRGC. (**b**) Index of sharpening at SPN (iS = DSi SPN / DSi2 DSRGC) for the case of two different ON-OFF DSRGCs which send simultaneous convergent inputs to the

postsynaptic cell. Presynaptic cells have different indices of selectivity, DSi1=0.46 and DSi2=0.58. The two cells have opposite preferred direction at 180° and 0°, respectively. The sharpening in direction selectivity in this case is much more restricted as in the case with two cells of the same preferred direction. iS>1 comprises also the areas with one of the synaptic strength equal to zero which leads to the monosynaptic case

Recently, important findings (Casti et al. 2008; Carandini et al. 2007; Sincich et al. 2007) suggest that at retinogeniculate synapse the variability in response of LGN cell is mainly due to intrinsic properties of retinal input and moreover, no special mechanism beyond simple summation of PSPs combined with spike threshold is necessary to accurately describe the LGN cell discharge as response to an incoming retinal input. It is beyond the scope of our work to validate a new model to characterize retinogeniculate transmission; instead we took advantage of the successfully validated model of Casti (Casti et al. 2008) and their simple approach used to describe the information processing between two first stages of the primary visual system, and investigated how information regarding direction of stimulus movement is shaped at the output of retina.

Sincich et al. (2007) have demonstrated that every spike within a burst at LGN neurons is generated by an EPSP evoked by a retinal spike. During bursts of rapid firing activity there are higher chances to observe more postsynaptic APs. Our simulation results show the same. Burst-like activity at preferred direction was responsible for a higher number of APs at SPN than at the intermediary directions (and thus sharpening of directional tuning). We found for all tested ON-OFF DSRGCs burst-like activity tuned at preferred direction, substantially higher than for ON DSRGCs. We therefore suggest that at preferred direction ON-OFF cells have a higher probability to successfully elicit an AP at postsynaptic target and thus to enhance the degree of direction selectivity. Recent evidences suggest also, that ISI preceding a retinal spike essentially influence the spike transmission at retinogeniculate synapse (Rathbun et al. 2007). In our simulations, when short ISI was present in the presynaptic spike trains, sharpening in directional tuning at

the postsynaptic counterpart was enhanced. At least in our simulation conditions, the key factor for a better signaling the direction of stimulus movement, from retina to higher brain areas, seems to be played by burst-like activity which is more accentuated in one type of DSRGCs known as ON-OFF type (Zeck and Masland 2007). This explains in part why in our simulations, monosynaptic excitatory connectivity between ON-OFF DSRGC and its postsynaptic target becomes the simplest scheme to achieve sharpening in direction selectivity.

We found that apparently, the presynaptic degree of directional tuning does not provide evidence how the sharpening works—we constructed artificial spike trains mimicking recorded DSRGCs and thus having the same directional tuning, but at the postsynaptic level we did not obtained similar iS for the artificial spike trains with the same DSi as the recorded cells. Instead, we found a more restricted parameter range for which sharpening can be achieved for these artificial spike trains. We then found that burst-like activity is less present in the artificial spike trains than in the recorded ON-OFF DSRGCs discharge. Moreover, ON-OFF DSRGCs show burst-like activity predominantly at preferred direction and less at intermediate directions of stimulus movement. The finding that each time the burst-like spiking activity at preferred direction was higher (as in the case of ON-OFF DSRGCs) we found the best sharpening in direction selectivity, lead us to the conclusion that this rapid firing activity at preferred direction of stimulus movement is the principal component of the spike train which carries the directional information. We varied most of the parameters involved in transformation of input spike train within the physiological plausible values. The output of all scenarios pointed toward the

same conclusion that the sharpening in direction selectivity was at its best when the component of the input spike train which carried the directional information—burst like spiking activity at preferred direction—was preserved and the components (isolated spikes) regarding stimulus direction at intermediary directions were lost in spike transmission.

As a conclusion of the above mentioned discussion upon the above mentioned results of our simulations we would like to strengthen the following remarks regarding burst-like activity:

1. Firstly, monosynaptic input was the simplest scheme, in our simulations, to achieve sharpening in direction selectivity at the output of DSRGCs.
2. We found sharpening for a larger parameters' values interval for ON-OFF DSRGCs than for ON DSRGCs.
3. Firing rate does not primordially explain the values obtained for the index of sharpening as we could notice from artificial spike trains mimicking DSRGCs with the same firing rate and DSi but showing different iS values.
4. To explain this discrepancy we focused on an intrinsic property of the retinal spike trains and thus we quantified the burst-like activity. We found that burst-like activity was larger for ON-OFF DSRGCs than for ON DSRGCs and artificial spike trains.
5. Burst-like activity was highly tuned at preferred direction for ON-OFF DSRGCs (DSi Burst > DSi Firing Rate) and thus increasing the chance to produce APs at the SPN at the preferred direction of stimulus motion.
6. Every time we found the best sharpening following parameters modification, we also had best burst-like activity effect upon the SPN.

That bursts are found at many synapses within the central nervous system is already well known (Sincich et al. 2007; Swadlow and Gusev 2001). It is also assumed that bursts are very important in transmitting important information at higher level within visual system (Usrey et al. 1999; Swadlow et al. 2002). In our case, presumably, their role is to signal the information regarding the direction of visual stimulus.

Once we learned out what component of retinal spike train is carrying the information about direction of stimulus movement, we asked how the simulated postsynaptic neuron does the enhancement of direction selectivity. The main effect responsible for the enhancement of direction-selectivity is presumably the spike threshold for the integrate-and-fire model and the cell's time constant, which determines the effect of temporal summation of PSPs. For slow input spike trains PSPs do not sum and the membrane potential of postsynaptic cell remains below the threshold.

Indeed we varied the spiking threshold ($V_{threshold}$) and we found that the sharpening in direction selectivity increased as the $V_{threshold}$ took higher values. At this high threshold values predominantly at preferred directions, EPSPs succeed to sum together in order to raise the membrane potential above and evoke APs at postsynaptic level. Postsynaptic cell's membrane time constant (τ_m) variation made even clearer the manner in which the enhancement of directional selectivity is performed. At low values of τ_m short ISI spiking activity is necessary so that EPSPs can sum and evoke APs at SPN level. Short ISI spiking activity is predominant at preferred direction enabling the temporal summation and thus increasing the sharpening. Once that τ_m increased the temporal summation was also possible for larger ISI too, commonly found for intermediary directions, so that we noticed a reduction in sharpening of direction selectivity.

That the enhancement of directional tuning at SPN is realized by the nonlinearity of the spike threshold applied with the temporal filter upon DSRGC spike train (combined with burst-like spiking activity at preferred direction) was more simply demonstrated by using an intuitive mathematical model consisting in a nonlinear amplifier, with a specific time constant, applied to ISI distribution of the retinal input spike train. We again found that if the temporal summation of PSPs was allowed only for small time constant than chances to have APs at SPN were greater at preferred directions (were short ISIs were predominant) and thus iS was largest.

Contribution of membrane potential threshold upon editing neuronal spike trains from presynaptic stage to postsynaptic level, has been intensively studied either for different neuron types, i.e. at retinogeniculate synapse (Casti et al. 2008; Carandini et al. 2007; Sincich et al. 2007), at geniculocortical synapse (Carandini and Ferster 2000; Jagadeesh et al. 1997; Priebe and Ferster 2005) or for different particularities of the visual stimulus presented to which recorded neurons are tuned, i.e. orientation selectivity (Volgushev et al. 2000; Carandini and Ferster 2000), direction selectivity (Jagadeesh et al. 1997; Volgushev et al. 2000; Carandini and Ferster 2000; Priebe and Ferster 2005). At both synapses, in order to account for the sharpening in direction selectivity, a nonlinear mechanism had to be taken into account (Priebe and Ferster 2008). For the direction selectivity, it is well known that cells in higher brain areas, i.e. primary visual cortex, are much more selective than cells in retina or LGN, so that V1 becomes an ideal stage to investigate sharpening in directional selectivity. In 1997 Jagadeesh et al., explained that enhancement of the direction selectivity of simple cells in V1 is generated at least in part by nonlinear mechanisms. Extracellular recordings from neuronal responses to moving stimulus could not be predicted accurately from linear combination of the

responses of stationary stimuli presented at different spatial positions within the cell's receptive field. To differentiate between several possible early nonlinear mechanisms, such as shunting inhibition, or PSP—to –spike transformation, i.e. spike threshold, intracellular recordings and a linear model of direction selectivity was used to analyze the synaptic potentials evoked by stationary sine-wave gratings. The direction selectivity of synaptic potentials was considerably smaller than that of the intracellularly recorded action potential indicating a non-linear mechanism such as threshold to enhance the direction selectivity of the cell's output over that of its synaptic input. Following Jagadeesh results, other scientific studies (Carandini and Ferster 2000; Priebe and Ferster 2005; Volgushev et al. 2000) remarked that spike threshold sharpens the direction selectivity in simple cortical cells evoking that spike threshold quantitatively accounts for the nonlinear component of direction selectivity amplifying the direction of selectivity of spike output relative to that of synaptic input. They have found that the spike threshold contributes substantially to the sharpening of directional tuning, creating a strong "iceberg effect" (Carandini and Ferster 2000).

Another related scientific result was that the degree of sharpening in individual cells was very different; sometimes a strong sharpening was created from poor directional tuning input and thus the degree of sharpening was high, and sometimes highly tuned cells provide little or no sharpening at the postsynaptic target (Volgushev et al. 2000). The sharpening was not correlated with resting membrane potential, threshold or optimal PSP amplitude and moreover was not cell type specific. Indeed we found this variation in degree of sharpening within the same cell type, ON-OFF DSRGCs. In our simulations we also found that the degree of sharpening of directional tuning is inversely related to the presynaptic DSi, that is, highly tuned presynaptic cells provided only small iS while low tuned presynaptic cells provided largest iS.

The model we used showed that for highly tuned ON-OFF DSRGCs, short ISI spiking activity is very concentrated at the preferred direction (Fig. 7(d)). For these cells we found less activity with large ISI even at non-preferred direction. Thus spike threshold mechanism altered very little to not at all the degree of directional tuning (iS was almost the same for $\tau=5$ ms as for $\tau=20$ ms). For low tuned presynaptic cells, we found many more isolated spikes (with large ISI) at non-preferred direction. Consequently, the temporal summation and spike threshold eliminated more isolated spikes at non-preferred directions and sharpens the directional tuning. Thus, we were able to measure higher iS for these cells. A comparison of the spike threshold effect in these two cases can be seen from Fig. 7 (c) (low tuned presynaptic cells) and Fig. 7(d) (highly tuned presynaptic cells).

Presumably for highly tuned cells, it is important rather to faithfully reproduce the information about the stimulus and thus the degree of sharpening is almost the same, while for low tuned cells it is strikingly important to better improve their directional tuning and thus to better transmit the information about the stimulus direction at the postsynaptic level (Volgushev et al. 2000).

When we varied most of the model parameters ($g_{max,e}$, $g_{max,i}$, τ_e) we noticed that their influence upon sharpening of direction selectivity, suggested two important parameters which characterize the temporal filter—$V_{threshold}$ and τ_m. Varying the other parameters the temporal summation of PSPs, spike threshold and burst-like activity at preferred direction of stimulus movement, were acting together to dictate the best sharpening in the manner above described.

In discrepancy with the ON-OFF DSRGCs, for the other type of direction selective cells, the ON DSRGCs, we found less sharpening at their postsynaptic counterparts under the same simulation conditions. This finding could be apparently at least counterintuitive since DSi for this cell type is lower than DSi for ON-OFF DSRGCs. However, the explanation is relatively simple and straightforward. For ON DSRGCs we found much less burst-like activity than for ON-OFF DSRGCs. Thus, the mechanism described above acting upon the incoming spike train, does not provide the same enhancement of iS since summation of PSPs at the preferred direction is not followed by a relatively high short ISI spiking activity in the ON DSRGC's spike train. To account for an eventual sharpening at the output of ON DSRGC (which project to the AOS) presumably the polysynaptic connectivity arrangement (Soodak and Simpson 1988; Ackert et al. 2006; He and Masland 1998; Oyster 1968) is more likely to sharpen directional tuning at the postsynaptic target.

Finally, we hypothetically checked how polysynaptic mechanism influences the degree of sharpening at the postsynaptic target. Interestingly, our simulations results show that two ON-OFF DSRGCs sending simultaneous excitatory synaptic input onto the same postsynaptic target lead to a better signaling of stimulus movement direction if they have the same preferred direction compared with the case when they have opposite preferred direction.

5 Conclusions

Using a simple approach, consisting in recorded DSRGCs inputs combined with a variant of a leaky integrate-and-fire neuron model and not taking into account neither synaptic plasticity nor cortical feedback input, we learned out that neurons postsynaptic to directional selective retinal ganglion cells signal better the direction of stimulus movement. We suggest that apparently, burst-like activity commonly found in

the ON-OFF DSRGCs is carrying the information regarding direction of stimulus movement toward higher brain areas. This intrinsic property of presynaptic input together with temporal filter and the nonlinearity of spike threshold at postsynaptic target, act upon the retinal input. The result is that the information regarding direction of stimulus movement at preferred direction is preserved while the component of incoming spike train, which signals direction of stimulus movement at non-preferred directions, is lost in the process of input spike train editing and thus the sharpening in direction selectivity is enhanced. Spike threshold act as a filter allowing that an AP is produced once that the threshold value of the membrane potential is reached. Summation has the effect that EPSPs reach the threshold. In order that summation to be efficient it is needed more closed in time EPSPs, situation which take place mostly during burst-like activity. This burst-like activity, for ON-OFF DSRGCs is distributed at preferred direction. Thus, PSP-to-spike transformation has maximum efficacy at preferred direction, at the other intermediate directions we will notice a reduction of spikes and thus the sharpening increases.

References

Ackert, J. M., Wu, S. H., Lee, J. C., Abrams, J., Hu, E. H., Perlman, I., et al. (2006). Light-induced changes in spike synchronization between coupled ON direction selective ganglion cells in the mammalian retina. *The Journal of Neuroscience, 26*(16), 4206–4215.

Alitto, H. J., & Usrey, W. M. (2005). Dynamic properties of thalamic neurons for vision. *Progress in Brain Research, 149*, 83–90.

Amthor, F. R., Takahashi, E. S., & Oyster, C. W. (1989). Morphologies of rabbit retinal ganglion cells with complex receptive fields. *The Journal of Comparative Neurology, 280* (1), 97–121.

Bair, W. (1999). Spike timing in the mammalian visual system. *Current Opinion in Neurobiology, 9*, 447–453.

Barlow, H. B., Hill, R. M., & Levick, W. R. (1964). Retinal ganglion cells responding selectively to direction and speed of image motion in the rabbit. *The Journal of Physiology, 173*, 377–407.

Barlow, H. B., Hill, R. M., & Levick, W. R. (1965). The mechanism of directionally selective units in rabbit's retina. *Journal of Physiology (London), 178*, 477.

Blitz, D. M., & Regehr, W. G. (2005). Timing and specificity of feed-forward inhibition within the LGN. *Neuron, 45*(6), 917–928.

Buhl, E. H., & Peichl, L. (1986). Morphology of rabbit retinal ganglion cells projecting to the medial terminal nucleus of the accessory optic system. *The Journal of Comparative Neurology, 253*(2), 163–174.

Carandini, M., & Ferster, D. (2000). Membrane potential and Firing rate in cat primary visual cortex. *The Journal of Neuroscience, 20* (1), 470–484.

Carandini, M., Horton, J. C., & Sincich, L. C. (2007). Thalamic filtering of retinal spike trains by postsynaptic summation. *Journal of Vision, 7*(14), 1–11.

Casti, A., Hayot, F., Xiao, Y., & Kaplan, E. (2008). A simple model of retina-LGN transmission. *Journal of Computational Neuroscience*. doi:10.1007/s10827-007-0053-7.

Cleland, B. G., & Lewick, W. R. (1974). Brisk and sluggish concentrically organized ganglion cells in the cat's retina. *The Journal of Physiology, 240*, 421–456.

Cleland, B. G., Lewick, W. R., Morstyn, R., & Wagner, H. G. (1976). Lateral geniculate relay of slowly conducting retinal afferents to cat visual cortex. *The Journal of Physiology, 255*, 299–320.

Damjanovic, I., Maximova, E., & Maximov, V. (2009). Receptive field sizes of direction-selective units in the fish tectum. *Journal of Integrative Neuroscience, 8*(1), 77–93.

Dann, J. F., & Buhl, E. H. (1987). Retinal ganglion cells projecting to the accessory optic system in the rat. *The Journal of Comparative Neurology, 262*(1), 141–158.

Devries, S. H., & Baylor, D. A. (1997). Mosaic arrangement of ganglion cell receptive fields in rabbit retina. *Journal of Neurophysiology, 78*(4), 2048–2060.

Godwin, D. W., Vaughan, J. W., & Sherman, S. M. (1996). Metabotropic glutamate receptors switch visual response mode of lateral geniculate nucleus cells from burst to tonic. *Journal of Neurophysiology, 76*, 1800–1816.

Grasse, K. L., Cynader, M. S., & Douglas, R. M. (1984). Alterations in response properties in the lateral and dorsal terminal nuclei of the cat accessory optic system following visual cortex lesions. *Experimental Brain Research, 55*(1), 69–80.

Guido, W., Lu, S. M., Vaughan, J. W., Godwin, D. W., & Sherman, S. M. (1995). Receiver operating characteristic (ROC) analysis of neurons in the cat's lateral geniculate nucleus during tonic and burst response mode. *Visual Neuroscience, 12*, 723–741.

He, S., & Masland, R. H. (1998). ON direction-selective ganglion cells in the rabbit retina: dendritic morphology and pattern of fasciculation. *Visual Neuroscience, 15*(2), 369–375.

Hoffmann, K. P., & Distler, C. (1989). Quantitative analysis of visual receptive fields of neurons in nucleus of the optic tract and dorsal terminal nucleus of the accessory optic tract in macaque monkey. *Journal of Neurophysiology, 62*(2), 416–428.

Huberman, A. D., Wei, W., Elstrott, J., Stafford, B. K., Feller, M. B., & Barres, B. A. (2009). Genetic identification of an On-Off direction- selective retinal ganglion cell subtype reveals a layer-specific subcortical map of posterior motion. doi:10.1016/j.neuron.2009.04.014.

Jack, J. J. B., Noble, D., & Tsien, R. W. (1975). *Electric current flow in excitable cells*. Oxford: Oxford University Press.

Jagadeesh, B., Wheat, H. S., Kontsevich, L. L., Tyler, C. R., & Ferster, D. (1997). Direction selectivity of synaptic potentials in simple cells of the cat visual cortex. *Journal of Neurophysiology, 78*, 2772–2789.

Jensen, R. J., & Devoe, R. D. (1983). Comparisons of directionally selective with other ganglion cells of turtle retina: intracellular recording and staining. *The Journal of Comparative Neurology, 17*(3), 271–287.

Kara, P. A., & Reid, R. C. (2003). Efficacy of retinal spikes in driving cortical responses. *The Journal of Neuroscience, 23*(24), 8547–8557.

Kim, I. J., Zhang, Y., Yamagata, M., Meister, M., & Sanes, J. R. (2008). Molecular identification of a retinal cell type that responds to upward motion. *Nature, 452*, 478–482.

Levick, W. R. (1967). Receptive fields and trigger features of ganglion cells in the visual streak of the rabbits retina. *The Journal of Physiology, 188*(3), 285–307.

Levick, W. R., Oyster, C. W., & Takahashi, E. (1969). Rabbit lateral geniculate nucleus: sharpener of directional information. *Science, 165*(3894), 712–714.

Lu, S. M., Guido, W., & Sherman, S. M. (1992). Effects of membrane voltage on receptive field properties of lateral geniculate neurons in the cat: contributions of the low-threshold Ca2 conductance. *Journal of Neurophysiology, 68*, 1285–1298.

Michael, C. R. (1966). Receptive fields of opponent color units in the optic nerve of the ground squirrel. *Science, 152*(3725), 1095–1097.

Mustari, M. J., & Fuchs, A. F. (1989). Response properties of single units in the lateral terminal nucleus of the accessory optic system in the behaving primate. *Journal of Neurophysiology, 61*(6), 1207–1220.

Oyster, C. W. (1968). The analysis of image motion by the rabbit retina. *The Journal of Physiology, 199*, 613–635.

Priebe, N., & Ferster, D. (2005). Direction selectivity of excitation and inhibitionin simple cells of the cat primary visual cortex. *Neuron, 45*, 133–145.

Priebe, N., & Ferster, D. (2008). Inhibition, spike threshold and stimulus selectivity in primary visual cortex. *Neuron*. doi:10.1016/j.neuron.2008.02.005.

Pu, M. L., & Amthor, F. R. (1990). Dendritic morphologies of retinal ganglion cells projecting to the nucleus of the optic tract in the rabbit. *The Journal of Comparative Neurology, 302*(3), 657–674.

Rall, W. (1967). Distinguishing theoretical synaptic potentials computed for different soma-dendritic distributions of synaptic inputs. *Journal of Neurophysiology, 30*, 1138–1168.

Rathbun, D. L., Alitto, H. J., Weyand, T. G., & Usrey, W. M. (2007). Interspike interval analysis of retinal ganglion cell receptive fields. *Journal of Neurophysiology, 98*, 911–919.

Sincich, L. C., Adams, D. L., Economides, J. R., & Horton, J. C. (2007). Transmission of spike trains at retinogeniculate synapse. *The Journal of Neuroscience, 27*(10), 2683–2692.

Soodak, R. E., & Simpson, J. I. (1988). The accessory optic system of rabbit. I. Basic visual response properties. *Journal of Neurophysiology, 60*, 2037–2054.

Stanford, L. R., & Sherman, S. M. (1984). Structure/function relationships of retinal ganglion cells in the cat. *Brain Research, 297*(2), 381–386.

Swadlow, H. A., & Gusev, A. G. (2001). The impact of "bursting" thalamic impulses at a neocortical synapse. *Nature Neuroscience, 4*, 402–408.

Swadlow, H. A., Gusev, A. G., & Bezdudnaya, T. (2002). Activation of a cortical column by a thalamocortical impulse (pdf). *The Journal of Neuroscience, 22*(17), 7766–7773.

Taylor, W. R., & Vaney, D. I. (2002). Diverse synaptic mechanisms generate direction selectivity in the rabbit retina. *The Journal of Neuroscience, 22*(17), 7712–7720.

Usrey, W. M. (2002). Spike timing and visual processing in the retinogeniculocortical pathway. *Philosophical Transactions of the Royal Society of London. Series B, Biological Sciences, 357*, 1729–1737.

Usrey, W. M., Reppas, J. B., & Reid, R. C. (1998). Paired-spike interactions and synaptic efficacy of retinal inputs to the thalamus. *Nature, 395*(6700), 384–387.

Usrey, W. M., Reppas, J. B., & Reid, R. C. (1999). Specificity and strength of retinogeniculate connections. *Journal of Neurophysiology, 82*, 3527–3540.

van der Togt, C., van der Want, J., & Schmidt, M. (1993). Segregation of direction selective neurons and synaptic organization of inhibitory intranuclear connections in the medial terminal nucleus of the rat: an electrophysiological and immunoelectron microscopical study. *The Journal of Comparative Neurology, 338*(2), 175–192.

Vaney, D. I., Levick, W. R., & Thibos, L. N. (1981a). Rabbit retinal ganglion cells. Receptive field classification and axonal conduction properties. *Experimental Brain Research, 44*(1), 27–33.

Vaney, D. I., Peichl, L., Wassle, H., & Illing, R. B. (1981b). Almost all ganglion cells in the rabbit retina project to the superior colliculus. *Brain Research, 212*(2), 447–453.

Volgushev, M., Pernberg, J., & Eysel, U. T. (2000). Comparision of the selectivity of the postsynaptic potentials and spike responses in cat visual cortex. *The European Journal of Neuroscience, 12*, 257–263.

Weng, S., Sun, W., & He, S. (2005). Identification of ON–OFF direction-selective ganglion cells in the mouse retina. *The Journal of Physiology, 562*(3), 915–923.

Wörgötter, F., & Koch, C. (1991). A detailed model of the primary visual pathway in the cat: comparison of afferent excitatory and intracortical inhibitory connection schemes for orientation selectivity. *The Journal of Neuroscience, 11*(7), 1959–1979.

Yonehara, K., Ishikane, H., Sakuta, H., Shintani, T., Nakamura-Yonehara, K., et al. (2009). Identification of retinal ganglion cells and their projections involved in central transmission of information about upward and downward image motion. *PLoS ONE, 4*(1), e4320.

Zeck, G. M., & Masland, R. H. (2007). Spike train signatures of retinal ganglion cell types. *The European Journal of Neuroscience, 26*, 367–380.